Pergamon International Journal of Machine Tools & Manufacture 39 (1999) 1157–1169

INTERNATIONAL JOURNAL OF MACHINE TOOLS & MANUFACTURE DESIGN, RESEARCH AND APPLICATION

Investigation of a 2-D planar motor based machine tool motion system

Michael A. Soltz, Y. Lawrence Yao*, Jehuda Ish-Shalom

Department of Mechanical Engineering, Columbia University, New York, NY 10027, USA

Received 15 July 1998

Abstract

A new 2-D planar motion system for precision machining operations is investigated. Characteristics of the 2-D planar motor system are studied to gain better understanding of its capabilities, limitations and interactions with machining processes. The planar motor system is applied to an end milling process, where experimental data on cutting force and surface finish are in agreement with simulation results. Of further interest is that the motor's fast response and ability to perform simultaneous motion in two directions potentially provides a simpler means to compensate for errors such as runouts. Issues associated with such compensation motions to improve surface finish are discussed. © 1999 Elsevier Science Ltd. All rights reserved.

Keywords: Sawyer motor; Linear motor; Machine tool; Motion system

1. Introduction

Machining is one of the most commonly used manufacturing processes. The machine tool industry continually strives to improve equipment performance, and provide alternative and innovative equipment [1]. The motion system of a machine tool plays an important role in achieving the required precision of a machining process. In addition, there often exist needs to compensate for inaccuracies stemming from other sources. An example is the adverse effect of runout in a milling operation on surface roughness. Increased surface roughness often leads to the need for a grinding finish, or simply increases the amount to be ground. To compensate for such effects, the lead screw/ball net based motion system is often incapable primarily because of its significant

* Corresponding author.

PII: S0890-6955(98)00085-6

inertia effects. Efforts have been made to compensate using a secondary motion system [2,3] and good results have been reported. The added complexity, however, may limit their industrial applications.

1.1. Proposed approach

A novel approach is proposed to replace the current lead screw system with a 2-D planar motor system. This system has a number of unique features: friction-free air-bearing system, fast response time and fine resolution. Perhaps the most significant advantage is the fact that a 2-D planar motor is capable of direct drive simultaneous motions in two directions. Not only would it be able to perform the current lead screw system's feed function, but it also would be able to provide additional planar X–Y motion which may be used to improve the surface quality. Thus a much simpler motion system is used (no coarse/fine double motion system needed). Since it is direct drive, backlash is basically eliminated. However, special considerations are needed for application of the motor to machining operations. Because the motor itself does not have the stiffness of the lead screw system, an appropriate control scheme is required. The limited maximum force of existing commercial motors limits its current use to medium to high precision machine tools where only relatively light cuts are involved.

1.2. Background

The 2-D planar motor, based on the Sawyer principle [4] to be briefly explained in the following section, has been used in the semi-conductor industry for wafer probing and also in X–Y plotters. Because of its compact size, high precision and speed, it is well suited for these environments. In these situations, no significant external forces are applied to the motor. The challenge for a machining operation is to control the motor in the presence of the external variable machining forces. Some previous work of applying direct drive to a machining process has been in the area of turning. Alter and Tsao [5,6] showed that direct drive can successfully be implemented and stability requirements can be met for a turning process. The next step in this development of direct drive motor use is not only to be able to compensate in one direction but simultaneously in two directions in addition to the feeding motion.

1.3. Objectives

Firstly, to study motor characteristics and investigate the system's capabilities and limitations. Nonlinearities inherent in the system are considered and dynamic characteristics are identified to verify simplifying assumptions. Other characteristics such as stiffness and resolution are also determined.

Secondly, to investigate application of the motor system to a machining operation. An end milling operation is chosen and the effect of runout is considered. Forces and surface profiles from experimental investigation are compared with simulation results.

Finally, to investigate the issues associated with simultaneous compensation and consideration of compensation strategies to improve surface quality.

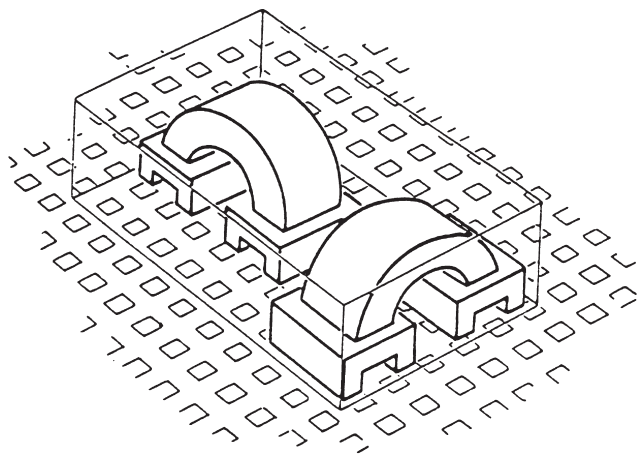

Fig. 1. Platen and two perpendicular forcers [7].

2. Planar motor system

A planar Sawyer motor [4] consists of two parts. A thin flat passive platen (stator) and a forcer (rotor). An air-bearing prevents frictional contact between the forcer and the platen. The friction of the moving part relative to the platen is reduced to the point that ultra-high resolution motion of 0.8 μin (20 nm) resolution with closed-loop feedback is available commercially using a laser position feedback.

The planar motor offers kinematic simplicity, modularity and a large planar motion range. The platen constrains the motor to the 3 DOF in a plane. The top thin steel plate of the platen of low carbon steel has groves cut in it at a fixed pitch (p = 0.020 inch for the motor used in this investigation), along both axes, to form a waffle pattern (Fig. 1).

2.1. Sawyer motor operation

A Sawyer planar motor is composed of at least two perpendicular linear motor forcers to obtain X–Y planar motion (Fig. 1). To obtain planar rotational control and higher stiffness, a third forcer is added to produce rotational torque in the plane. Thus the motor we used has one central Y linear forcer and two parallel X linear forcers spaced 11.2 in apart. Fig. 2 shows the principle of operation of a two phase 1 DOF linear motion forcer [4]. Each linear forcer is composed of two identical phases M^0 and M^{90} offset by (1/4 + n) tooth pitch, n = integer. An intuitive explanation of motor's operation is given here; a detailed magnetic model is given in [7].

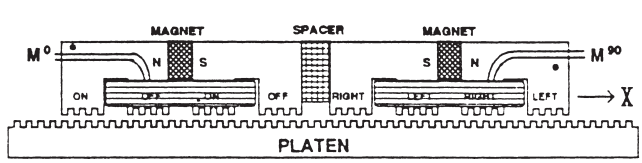

Fig. 2. Linear Sawyer forcer principle [8].

We start with the motor at the position shown in Fig. 2, with no currents. The M^0 phase magnet produces magnetic flux that closes through the aligned poles labeled ON, since the poles' teeth are aligned with the platen teeth. In contrast, the OFF poles' teeth are misaligned and thus a smaller amount of flux closes through them. In the M^{90} phase all four poles are 'half' misaligned and the flux distributes evenly between the RIGHT and LEFT poles (ignoring edge effects). At this position the net lateral X force is zero, since M^0 has zero net force from each pole and in M^{90} the RIGHT and LEFT forces balanced.

By increasing the current in M^{90} while decreasing the current in M^0 to zero, the platen will move 1/4 cycle in the + X direction. To continue to move another 1/4 cycle + X, one would apply the same principle, i.e., increase the current in M^0 while decreasing the current in M^{90} to zero. With two more steps, applying current in the negative polarity, the motor would move one whole tooth pitch distance and return to the same pole arrangement started with in Fig. 2.

With a 508 μm (20 mil) tooth pitch motor, this full step resolution is 127 μm (5 mil). Finer position resolution is achieved by 'μ-stepping,' i.e., interpolating the currents so that the net balance of forces between the two motor phases M^0 and M^{90} gives a very large set of equilibrium points (beyond the four discussed before). Using open-loop μ-stepping 'control,' the 508 μm pitch motor above can achieve 0.5 μm (0.02 mil) resolution. The 'magnetic internal position closed-loop' can achieve high stiffness, 3000 lb/inch, leading to good position performance, even when using just μ-stepping with 'external' open-loop control.

Using a Sawyer sensor [8] the motor can be electronically commutated to eliminate the multiple equilibrium points existing in μ-stepping control. The Sawyer sensor can also be used to obtain much higher motor stiffness by closed-loop control [8].

3. Dynamic characterization

The relationship between the magnetic force exerted by the forcer and its displacement relative to the platen for a given equilibrium position is depicted in Fig. 3.

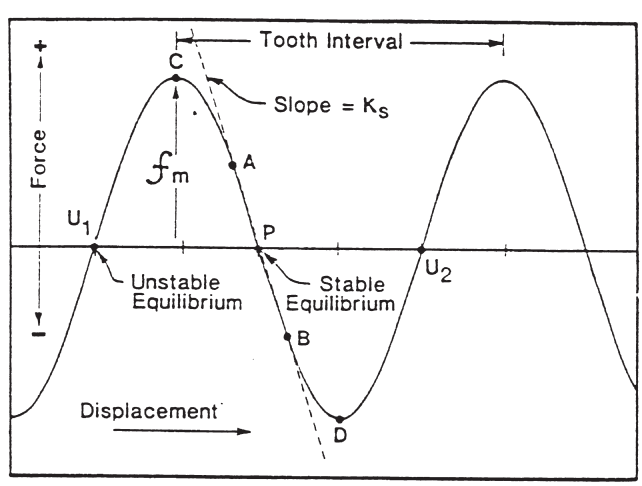

Fig. 3. Motor force vs displacement [13].

Therefore, the equation of motion relating commanded position $c(t)$ to response $r(t)$ along the X or Y axis can be expressed as:

$$m\ddot{r}(t) + k_v\dot{r}(t) = f_m \sin\left[\frac{2\pi(r(t) - c(t))}{p}\right] \tag{1}$$

where m = mass of forcer and load, k_v = drag (damping) coefficient, f_m = maximum force and p = tooth pitch (cycle) of platen.

As the forcer moves over the platen, eddy currents are induced which create a drag force that is nearly proportional to velocity. Thus the sinusoidal force-vs-displacement term is the only nonlinear term in Eq. (1). The sinusoid may be replaced by a constant k_s if the displacement is within a range of say one tenth of a tooth interval ($\pm$ 1 mil), that is, between points A and B (Fig. 3). Under these assumptions Eq. (1) can be approximated by:

$$m\ddot{r}(t) + k_v\dot{r}(t) + k_s(c(t) - r(t)) = 0 \tag{2}$$

A series of experiments were performed on the motor to be used in this investigation to determine its dynamic characteristics and verify the linear approximation. A laser interferometer system with a resolution of 6 μin (0.16 μm) was used to measure the impulse response of the motor. The experiments were performed for both the X and Y directions. Fig. 4(a) shows the impulse response of the motor in the X direction and Fig. 4(b) the corresponding frequency plot.

From the frequency plot a natural frequency of about 65 Hz is found with a damping ratio of about 0.02. Similarly for the Y axis, a natural frequency of 48 Hz and with a damping ratio of also about 0.02. The original controller of the motor had a back EMF feedback circuit to increase the damping of the motor at the end of a move. Fig. 5 shows the impulse response of the motor with the damping on. With the damping added the value of damping ratio increased to over 0.2 for large motions. The static stiffness of the motor was also measured using the laser interferometer and a spring loader. Using a simple relationship,

$$F = -k(x = x_d) \tag{3}$$

where F = force applied, k = unknown spring constant (stiffness), x = measured displacement and x_d = desired position of motor.

The stiffness in the X direction was found to be 3300 lbf/in, while in the Y direction the stiffness was 1800 lbf/in. The mass of the forcer platen protection shield and load was about 6 lb. The motor has a tooth pitch (cycle) of 0.02 with a μ-stepping resolution is about 20 μin (0.5 μm), Fig. 6, using the PC controller in Fig. 7. The PC controller replaced the original controller and will be explained in a later section.

4. Application of the motor

The aforementioned characterization of the motor determined its capabilities and limitations. It has a relatively high natural frequency and good resolution, but may be limited by the amount of stiffness and damping available. To investigate its interaction with machining, the motor is applied to a machining operation. The milling process is chosen because it could most benefit

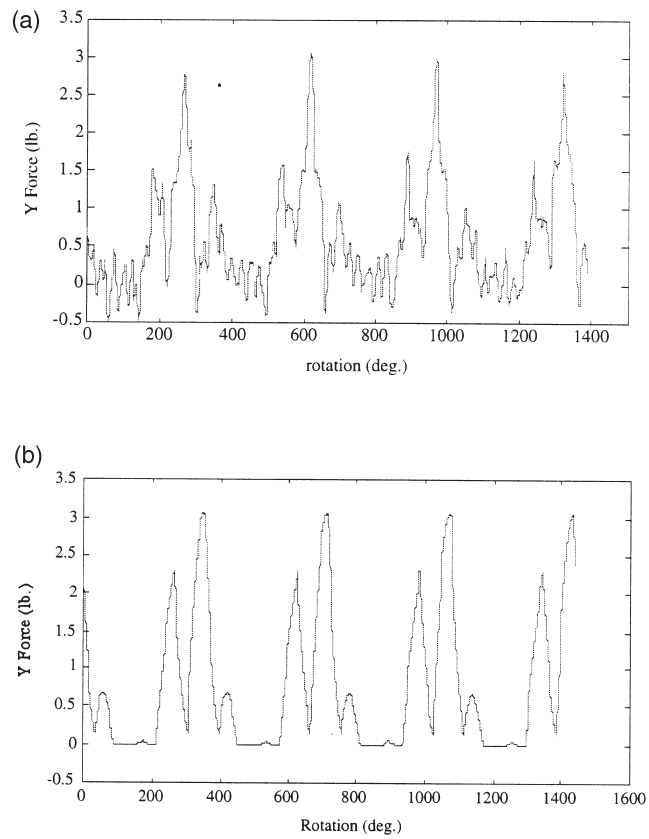

Fig. 4. (a) Impulse response of the motor. (b) Corresponding frequency response.

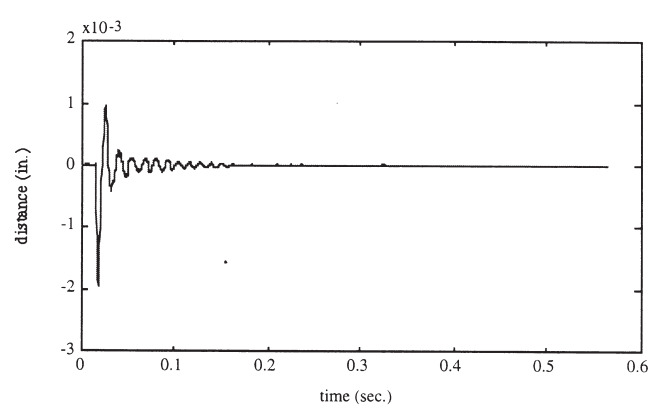

Fig. 5. Impulse response with added damping.

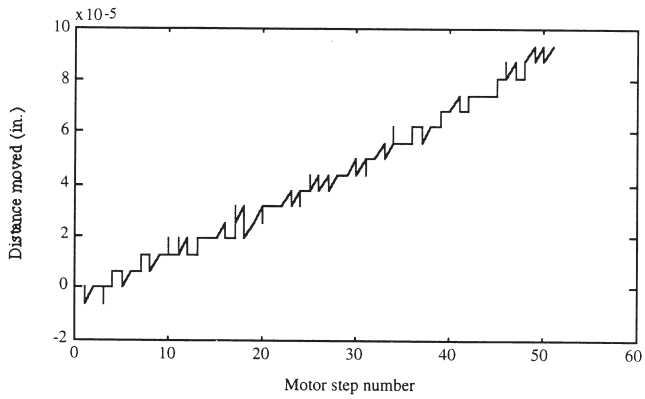

Fig. 6. Stepping resolution.

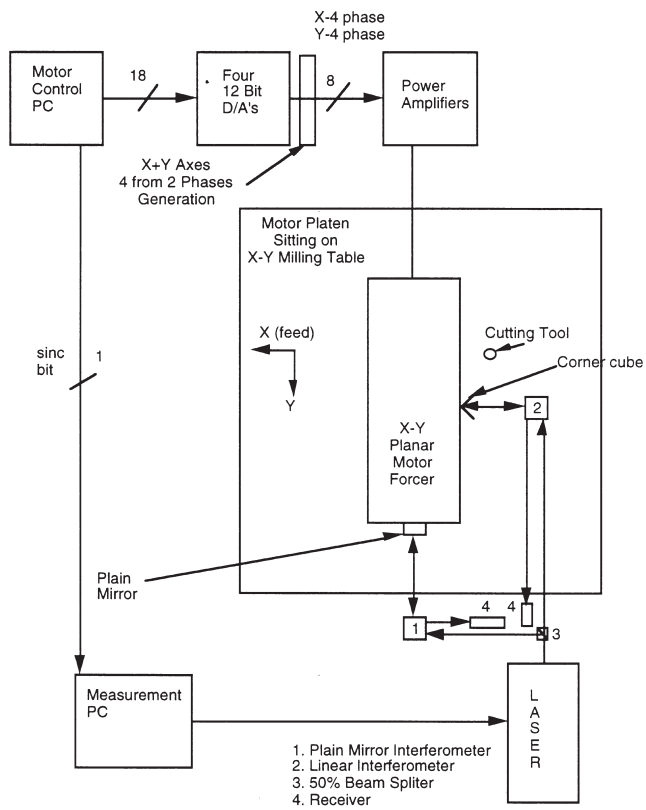

Fig. 7. System layout.

from the 2-D simultaneous motion capability of the motor. Such compensation capability is highly desirable to improve poor surface finish and reduce tool wear caused by runout. Specifically, the end milling process was chosen where it is more convenient to characterize the runout and thus offers simplicity for initial attempts.

Much work has been done on the end milling process to model the force system [9,10] and the surface generation [11,12]. Because milling is an interrupted cutting process, the forces pulsate as each tooth is engaged. This further causes periodic tool deflection resulting in poorer surface quality. The most significant effect in multi tooth cutting systems is runout. For end milling, runout can be caused by any number of things, but usually it is due to axis offset. A simulation model [10] to predict cutting forces under these imperfections is adapted in this paper.

The prediction of surface generated was done using the method developed by Babin et al. [11,12]. Although tool deflection can play an important role in surface quality, it is not considered in this case. Our approach is to concentrate on motor stiffness which is less than the stiffness of the cutter. Therefore the interactions between the motor and the cutting process need to be investigated. They can be expressed as

$$m\ddot{x}(t) + k_{vx}\dot{x}(t) + k_{sx}(c_x(t) - x(t)) = f_x(t) \tag{4}$$

$$m\ddot{y}(t) + k_{vy}\dot{y}(t) - k_{sy}y(t) = f_y(t) \tag{5}$$

where X is the direction of feed and $c_x(t)$ the commanded feed. $f_x(t)$ and $f_y(t)$ are instantaneous cutting forces in X and Y directions, respectively. If the inertial and damping terms are smaller than the spring term, static relationships may suffice. This will be discussed further in the Experimental section of the paper.

5. Experimental investigation

Experiments were performed to verify the relation of the simulation to experimental data and to show the viability of using this motor in a milling operation.

5.1. Experimental setup

Experiments were done using the system block diagram outlined in Fig. 7. Motor control was performed by a PC. A movement program was developed to deliver the required control currents to the X and Y motor's coils. Two phase (sin() and cos() waves) digital commands were generated for both the X and Y axes. These commands were sent to an AD390 chip that contains four 12 bit digital-to-analog converters which were updated simultaneously. Since each motor axis is controlled by four coils the two phase analog signals (sin() and cos() waves) were added and subtracted to give the required four phases to the motor's coils. The existing motor controller was bypassed and only its eight power amplifiers were used. The two, X axis motor sections' coils, are connected in parallel. No control is provided in this case for motor planar rotation.

A laser interferometer was used to measure both position and force. Force was measured by converting the displacement measurement using Eq. (3). The laser position measurement resolution was along the X axis 6 μin (0.16 μm) and 3 μin (0.08 μm) along the Y axis. Y axis resolution is better since it uses a plane mirror interferometer compared to a linear interferometer along the X axis. Surface measurements were done using a Taylor/Hobson Talysurf surface measuring machine. Fig. 8 shows the actual setup.

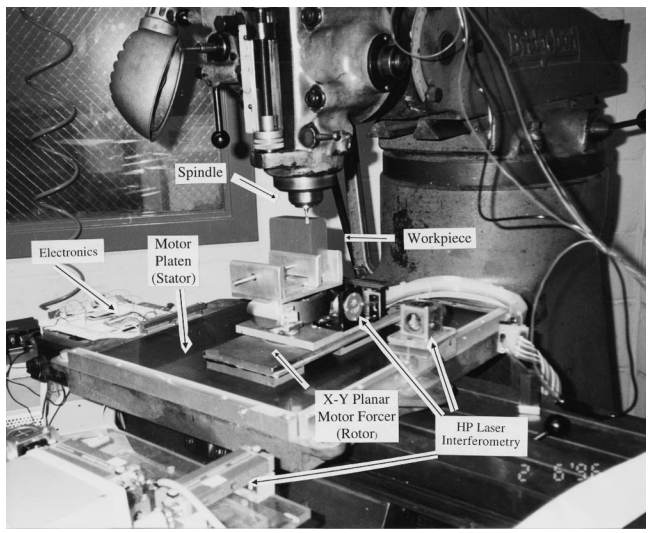

Fig. 8. Experiment setup.

5.2. Experimental conditions

Experiments were performed on a Bridgeport milling machine using a 0.1875 in. diameter, 30 degree helix angle, 4 fluted end mill. The effective length of the end mill was 0.875 in. The workpiece material selected was a machinable wax. A vice was constructed to securely hold the work material. Considerations were taken so as to insure that the vice was well secured on top the motor. All tests were done at a feed rate of 2 in/min and cutting tool rotation speed of 135 rpm. Axial depth of cut (AD) of 0.15 and 0.25 in., and radial depth of cut (RD) of 0.04 and 0.08 in. were varied in a 2^2 factorial design. Therefore four different conditions were used in experiments.

5.3. Comparison with simulation

The model for the end milling process requires a fit of two parameter to actual data, that is, computation of the constants K_t and K_r [9]. For this, the system is assumed to be rigid. Displacement data from cutting was used to estimate the average force. Since the cutting speed used was low, the motor dynamics (inertial and damping forces) could be neglected. This was verified by taking numerical derivatives of the displacement data and using Eq. (2).

The mass and damping coefficient were measured to be 0.0207 lbm and 0.217 lbm/s. The calculated inertial and damping force were then found to be on the order of 0.5×10^{-3} lbf, which was much less than the static force, on the order of 1–2 lbf.

The cutting data was analyzed. The results are presented below. Fig. 9(a, b) are actual versus simulated forces for an axial depth of cut 0.15 in and radial depth of cut of 0.04 in. Fig. 9(a) shows a varying force. After inspection of the milling system it was found the spindle had an inherent runout of about 0.5 mil. This value was used in the simulation and the results are shown in Fig. 9(b). There is a reasonable agreement between the simulation and actual data. Peak forces

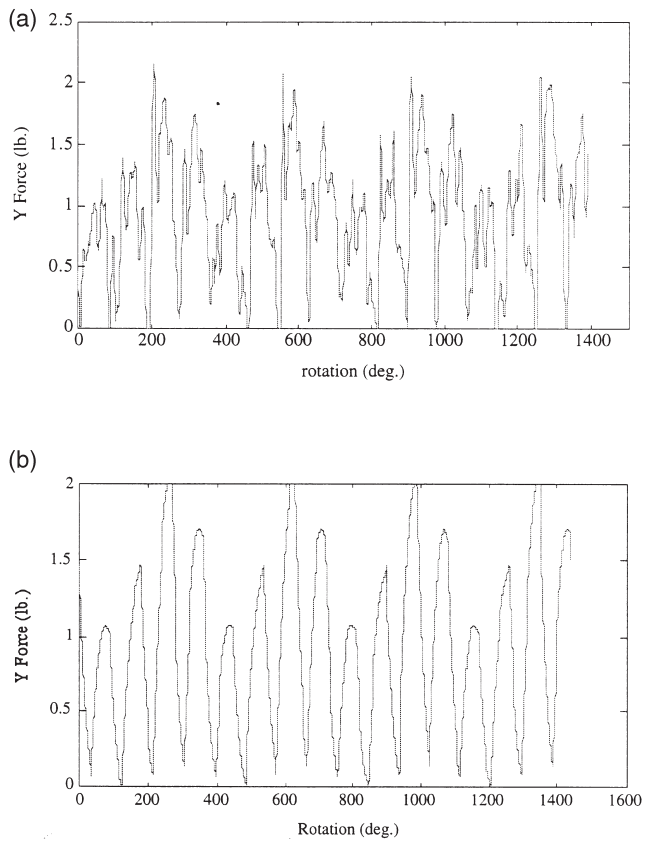

Fig. 9. (a) Experimental cutting force. (b) Simulated cutting force. For both: AD = 0.15 in., RD = 0.04 in., runout of 0.5 mil.

are about the same for actual data for simulated. The frequency corresponds to the tooth passing frequency of 9 Hz.

A shim was placed in the tool chuck to simulate a cutter offset of 3 mil. Fig. 10(a, b) shows actual and simulated data for an axial depth of 0.15 in. and 0.04 in. radial depth. The agreement is fairly good. The general trend of the data is very similar and peak forces were about the same for actual and simulated data respectively. The simulated surface for the above condition is presented below. There is reasonable agreement between the actual data (Fig. 11(a)) and simulation (Fig. 11(b)).

5.4. Discussion

Experiments showed that the motor system is capable of machining applications, especially for medium to high precision applications where only light cuts are required. The particular motor used is limited by its maximum force and stiffness. Motors with larger forces are available and prototype motors with much larger force of 900 lbf were built. Because this motor is typically used in a specialized industry, i.e. the semiconductor industry, it is relatively costly. However, if

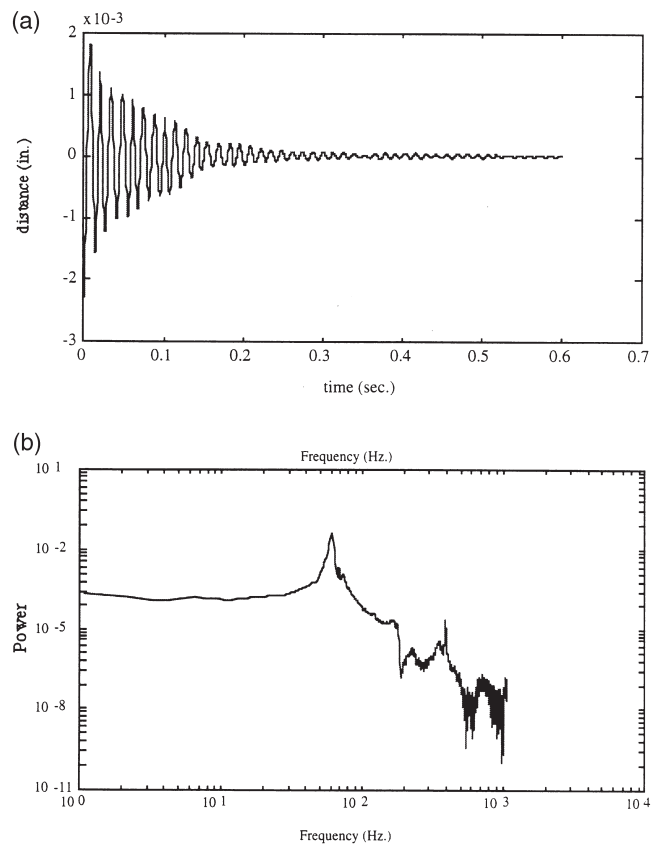

Fig. 10. (a) Experimental cutting force. (b) Simulated cutting force. For both: AD = 0.15 in., RD = 0.04 in., runout = 3 mil.

the machine were to be produced in a larger quantity, costs should decrease. In terms of application to a mill, the motor requires a shield to keep chips and debris from falling on the platen. This could be resolved though by creating a type of flexible apron to cover the platen as it moves.

6. Error compensation issues

The motor's fast response and ability for simultaneous X–Y motion can be utilized to compensate for adverse effects of errors such as runouts on surface roughness. Since the spring term is dominant as mentioned before, an intuitive approach is to basically follow the runout, i.e., have a sinusoidal motion in both the X and Y directions while still feeding at a constant rate. It is important to note that only this type of motor has the capability to do a motion such as this. The lead screw does not have the response rate needed. This idea can also be applied to contour cutting in which the motor would feed in two directions while simultaneously do a compensation motion.

In doing so, compensation needs to be well synchronized with the angular position and thus a spindle encoder system has been implemented. Otherwise, slight difference between the compen-

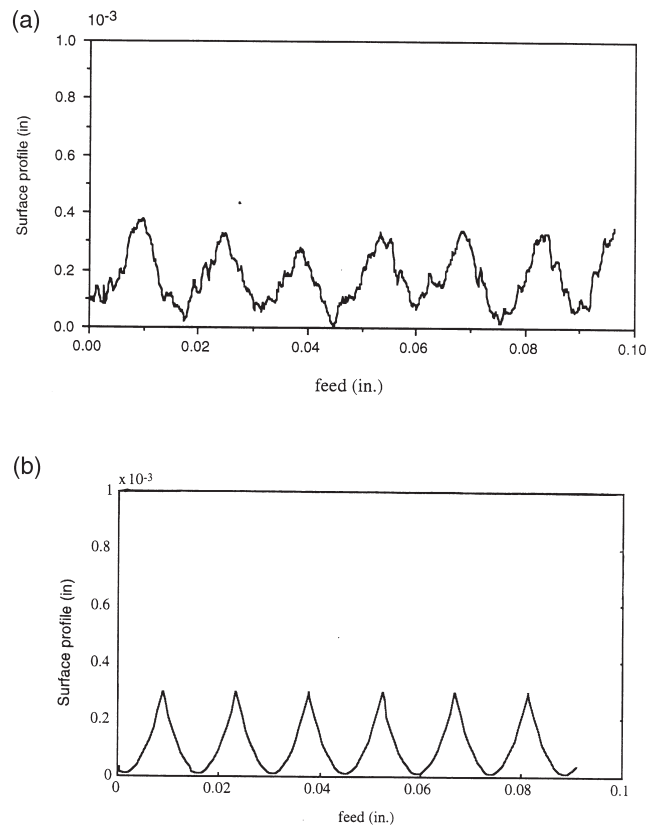

Fig. 11. (a) Surface generated (talysurf measurement). (b) Surface generated (simulation). For both: AD = 0.15 in., RD = 0.04 in., runout = 3 mil.

sation frequency and the runout frequency (the same as that of the spindle which may be time varying) will cause beating. Very initial results show that this method is feasible, but this approach needs to be further tested. One big advantage of this method is that only spindle angle needs to be measured and used for runout compensation and no need for force measurement. This simplifies the system.

A better opportunity would be to use a feedback control which would increase stiffness of the motor system. The position sensor used is limited in that, because the laser is external to the system, it is not practical for machining. An internal high resolution position sensor (0.2 μm) such as the one presented in Ish-Shalom [8] would be needed. Using this internal position sensor the motor can be operated as a brushless d.c. motor with electronic commutation from the sensor. Using electronic commutation allows one to utilize the maximum motor force for machining and the problematic cyclic term sin() in Eq. (1) is removed. Therefore with electronic commutation the motor does not exhibit any loss of sync condition which is very important for reliable operation of the system. Using a pair of internal sensors along the same axis with a given displacement (like the X axis motor sections) the planar motion rotation degree-of-freedom can be sensed and using closed-loop control can be controlled to have higher stiffness as well.

7. Concluding remarks

A new 2-D machine tool motion system is investigated. It has the following advantages over the current lead screw system: friction-free air-bearing system, fast response time, high resolution, compact in size, and most importantly has the capability of simultaneous direct drive X–Y motion. This system has the potential to improve surface finish of machined parts, as discussed for the end milling process. The relevant issues associated with error compensation applications are discussed.

Acknowledgement

Assistance by Dr W. Li in experimental measurements is gratefully appreciated.

References

[1] S.M. Wang, K.F. Ehmann, Error model and accuracy analysis of a six-DOF Steward platform, Manufacturing Science and Engineering ASME MED 2–1 (1995) 519–530.
[2] S.Y. Liang, S.A. Perry, In-process compensation for milling cutter runout via chip load manipulation, J. Engineering for Industry 116 (1994) 153–160.
[3] K. Kim, K.F. Eman, S.M. Wu, In-process control of cylindricity in boring operations, ASME Trans. J. Engineering for Industry 109 (1987) 291–296.
[4] B.A. Sawyer, Magnetic Positioning Device, US patent 3,457,482, 1969.
[5] D.M. Alter, T.C. Tsao, Dynamic control of the turning process using direct drive linear motor actuators, in: Proceedings of the American Control Conference, Chicago, IL, 1992, American Automatic Control Council, Green Valley, AZ, pp. 379–383.
[6] D.M. Alter, T.C. Tsao, Implementation of a direct drive linear motor actuator for dynamic control of the turning process, in: Proceedings of the American Control Conference, San Francisco, CA, 1993, IEEE, Piscataway, NJ, pp. 1971–1975.
[7] W.E. Hinds, B. Nocito, The Sawyer linear motor, in: B.C. Kuo (Ed.), Theory and Application of Step Motors, West Publishing Co., 1973, pp. 327–339.
[8] J. Ish-Shalom, Sawyer sensor for planar motion system, in: Proc. IEEE International Conf. on Robotics and Automation, San Diego, May, 1994, IEEE, Piscataway, NJ, pp. 2652–2658.
[9] W.A. Kline, R.E. DeVor, The effect of runout on cutting geometry and forces in end milling, Int. J. Mach. Tool Des. Res. 23 (1983) 123–140.
[10] W.A. Kline, R.E. DeVor, J.R. Lindberg, Prediction of cutting forces in end milling with application to cornering cuts, Int. J. Mach. Tool Des. Res. 22 (1982) 7–22.
[11] T.S. Babin, J.M. Lee, J.W. Sutherland, S.G. Kapoor, A model for end milled surface topography, in: Proc. 13th NAMRC, 1985, pp. 362–368.
[12] T.S. Babin, J.W. Sutherland, S.G. Kapoor, On the geometry of end milled surface, in: Proc. 14th NAMRC, 1986, Society of Manufacturing Engineers, Dearborn, MI, pp. 168–175.
[13] J. Nordquist, P. Smit, A motion control system for (linear) stepper motor, Incremental Motion Society, 1985, The Incremental Motion Control Systems Society, Champaign, IL, pp. 215–231.